

Improving the Resolution in Direct Inductive Sensor-to-Microcontroller Interface

Zivko Kokolanski, Ferran Reverter, Cvetan Gavrovski and Vladimir Dimcev

Abstract – The paper describes an improved direct inductive sensor to microcontroller interface by incorporating external MOSFET transistors. In such a way, the measured discharging time interval can be increased (through the discharging time constant) which results in increased resolution for a given time base. The experimental results show that the resolution of the measurements can be significantly improved in comparison to the basic low pass filter and high pass filter topology. Moreover, such circuit can be used to interface inductive sensors with lower inductance.

Keywords – Inductive sensor, microcontroller, sensor interface, resolution

I. INTRODUCTION

Inductive sensors are widely used to measure position, speed, displacement, vibration, and other process variables, especially in harsh environments [1]. Generally, a change in the process variable is reflected into variation of the inductance of the sensor. In order to obtain a useful signal from such sensors to embedded systems such as microcontrollers, usually a combination of signal conditioning electronic circuits in between the sensor and the microcontroller are used [2]. The signal conditioning circuits are usually performing some of the following tasks: 1. Inductance-to-alternating current (AC) voltage conversion, root mean square (RMS)-to-direct current (DC) voltage conversion and analog-to-digital (AD) conversion; or 2. Inductance-to-frequency conversion and logic level translation. Such complex signal conditioning increases the space, cost and power consumption.

In recent years, several interface circuits for inductive sensors with direct digital output were proposed [3]-[6], thus eliminating the need of AD converter. The interface circuit can be simplified even more by means of direct sensor-to-microcontroller interface. In the last decade, a lot of papers have been published on direct interface for resistive and capacitive sensors [7], as well as their differential [8], [9] and bridge configurations [10]. Recently the direct interface was also applied to inductive sensors in low pass filter (LPF) topology [11]-[13] given in Fig. 1, and high passes filter (HPF) topology [14], [15] given in Fig. 2. In both cases, a microcontroller is used to excite the RL/LR circuits and measure its transient response (charging/discharging time) through the sensor (L_x) and the calibration (L_c) inductance. Afterwards, a single point calibration is used to estimate the sensor inductance.

Z. Kokolanski, C. Gavrovski and V. Dimcev are with the Department of Electrical Measurements and Matherials, Faculty of Electrical Engineering and Information Technologies, Ss. Cyril and Methodius University in Skopje, Rugjer Boskovic 18, 1000 Skopje, Macedonia, e-mail: kokolanski@feit.ukim.edu.mk

F. Reverter is with the Department of Electronic Engineering, Universitat Politècnica de Catalunya-BarcelonaTech, C/ Esteve Terradas 7, 08860 Castelldefels (Barcelona), Spain

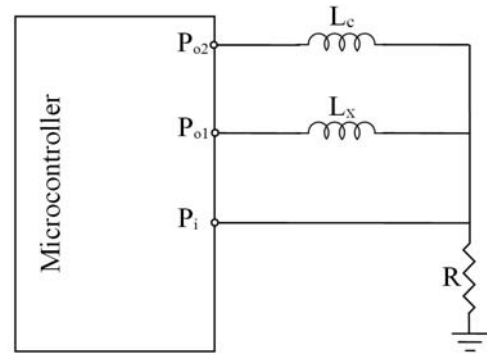


Fig. 1. Direct inductive sensor-to-microcontroller interface in low pass filter (LPF) topology

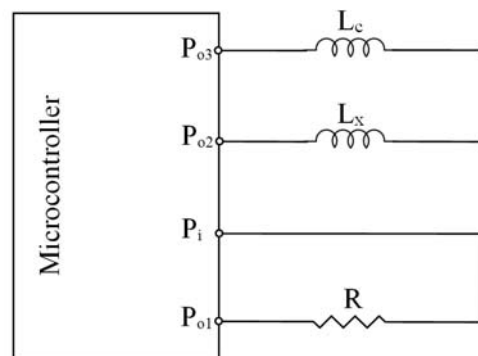


Fig. 2. Direct inductive sensor-to-microcontroller interface in high pass filter (HPF) topology

However, one of the major restrictive factors in both LPF and HPF circuit topologies is the microcontroller's maximal output current sink/source capability (typically around 20-30 mA) which limits the minimal external resistor R value, and consequently limits the charging/discharging time constant. In this context, the HPF is advantageous over the LPF topology and offers a larger time constant, i.e. higher resolution for a given time base (at the expense of more microcontroller interface pins). Nevertheless, for typical microcontroller clock frequencies up to 20 MHz, the measurements are roughly restricted to the millihenries range which rigorously limits the application to different inductive sensors. In this paper, a possibility to increase the discharging time constant with external MOSFET transistors (thus, increase the resolution) is given.

II. OPERATING PRINCIPLE

The modified direct sensor-to-microcontroller interface circuit in HPF topology with external MOSFET transistors is given in Fig.3. The circuit uses three N-channel (T_1 - T_3) and one P-channel (T_4) MOSFET transistors in between the passive network and the microcontroller. According to the

measurement procedure, two RL circuits are formed: circuit formed by R and L_x , and one formed by R and the reference inductor L_c . Each RL circuit is measured in two phases (first and second phase). The state of the microcontroller pins during the first and the second phase are given in Fig. 4 and Fig. 5 respectively. In the first phase of the RL circuit formed by R and L_x , the port P_{o1} is in a logical “0” state (turning off T_1), the port P_{o2} generates a logical “1” (turning on T_2), the port P_{o3} is in a logical “0” (turning off T_3 and turning on T_4), and the port P_i is configured as “input”. In such a way, the microcontroller generates a transient pulse (through the MOSFET “driving” circuit) at the input of the RL_x circuit. In the meanwhile the microcontroller measures (with the built in timer) the discharging interval (exponential discharging voltage from the power supply voltage V_{dd} to the lower threshold voltage V_{il} of P_i) seen by the input port P_i . Afterwards, the microcontroller ports are configured for the second phase as given in Fig. 5. Now the transistor T_4 is “off” and T_3 is “on” discharging the stored energy in L_x through R . The second phase lasts typically 7÷9 times the time constant ($\approx L_x/R$). The first and the second phase of the RL circuit formed by R and L_c are performed similarly (only the transistor T_1 is on and T_2 is off). The voltage waveforms of the characteristic signals during the measurements are given in Fig. 6. Hence, the sensor inductance is then estimated by using the single point calibration as:

$$L_x = \frac{t_x}{t_c} L_c, \quad (1)$$

where t_x is the measured discharging time interval through L_x , and t_c is the measured discharging interval through L_c . Note that the duration of the time intervals t_x and t_c are proportional to the time constants L_x/R and L_c/R respectively. It is clear that the time constants can be increased by decreasing the value of R . However, R is limited by the maximal drain current of the MOSFET transistors (I_d) and by the maximal allowed peak current through the sensor (I_p) so that

$$\frac{V_{dd}}{R + 2R_{dson}} \leq I_d, I_p, \quad (2)$$

where it is assumed that $R_{dson1}=R_{dson2}=R_{dson3}=R_{dson}$ (R_{dson} is the drain to source ON-resistance of the N-channel MOSFET transistors T_1 - T_3). The current technology easily offers small-size MOSFET transistors with drain currents in the order of amperes, whereas the output sink/source currents of the microcontroller ports are in the order of milliamperes. Therefore, the modified interface circuit allows using much lower value of the external resistor R (comparing to the circuits given in Fig.1 and Fig.2), limited mainly by the maximal allowed peak current through the sensor I_p . For a given time base, this will result in increased measurement resolution.

III. EVALUATION OF THE MEASUREMENT RESOLUTION

According (1) it is clear that the resolution of the measurements is mainly limited by the quantization of the timer in the microcontroller when measuring t_x and t_c .

Hence, the resolution of the time-to-digital conversion can be expressed, assuming only quantization effects, as:

$$N = \log_2 \left(\frac{t_{xmax} - t_{xmin}}{T_0} \right), \quad (3)$$

where t_{xmax} and t_{xmin} are the discharging time intervals for the maximal and the minimal sensor inductance respectively, and T_0 is the effective time base of the timer.

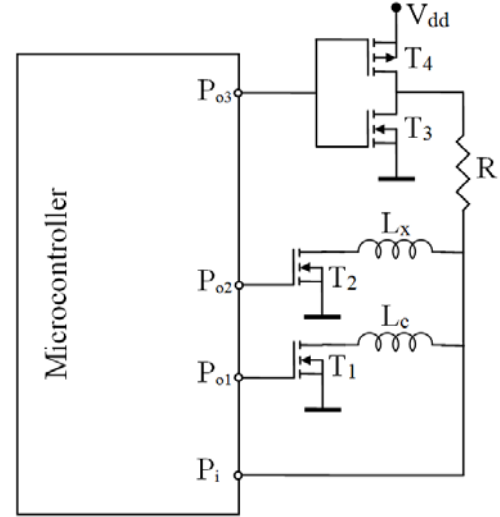


Fig. 3. Improving the time constants of the inductive sensor interface circuit with external MOSFET transistors

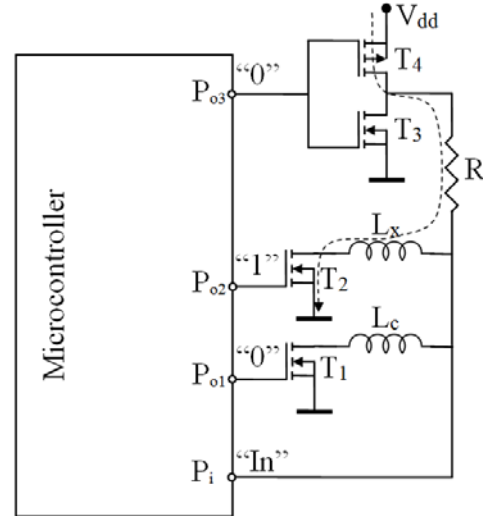


Fig. 4. State of the microcontroller pins during the “first” phase of the inductive sensor interface circuit

However, the measurement also suffers from trigger noise effects, thus decreasing the resolution. The effective number of bits (ENOB) of resolution can be expressed, assuming both quantization and trigger noise effects, as:

$$ENOB = N - \log_2 \left(\frac{\left| \sqrt{u_q^2 + u_n^2} \right|_{\max}}{u_q} \right), \quad (4)$$

where u_q is the quantization uncertainty, and u_n is the uncertainty due to noise effects. In direct sensor-to-

microcontroller interface the start of the measurement is synchronous with the timer, therefore according [16] the quantization uncertainty is given with:

$$u_q = \frac{T_0}{2\sqrt{3}} \quad (5)$$

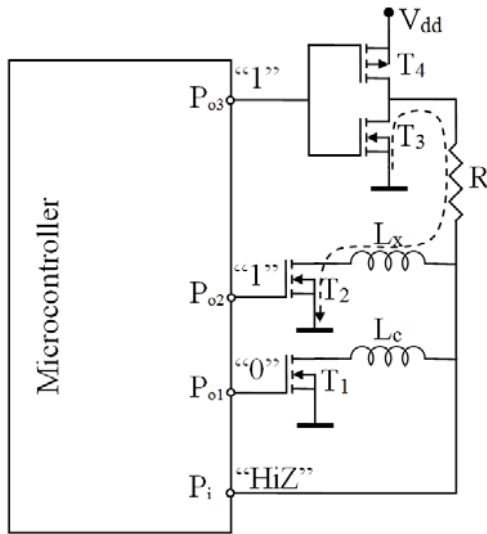


Fig. 5. State of the microcontroller pins during the “second” phase of the inductive sensor interface circuit

The noise related uncertainty is usually not defined in the microcontroller datasheet, therefore it can be evaluated by using a Type A evaluation, i.e. by statistical analysis of series of observations, given with:

$$u_n = \pm \frac{\sigma}{\sqrt{n}}, \quad (6)$$

where σ is the standard deviation of n consecutive readings of t_x .

IV. EXPERIMENTAL RESULTS AND DISCUSSION

The experiments were performed by using a general purpose 8-bit microcontroller PIC16F877A with clock frequency of 20 MHz. A prototype board capable for

implementation of all direct inductive sensor-to-microcontroller topologies (HPF, LPF and HPF with MOSFET transistors) was designed. The prototype board is given in Fig. 7. To reduce the noise effects, a special attention was paid to designing printed circuit board (PCB) ground plane and power supply decoupling. To emulate the extreme points of an inductive sensor, a decade inductance box was used. The minimal sensor inductance was 1 mH and the maximum inductance was 9 mH (for inductive sensors like [17]).

According to the manufacturer datasheets, the maximum output current sink/source for PIC16F877A is 25 mA. Hence, having in mind the implementation conditions for achieving maximal resolution, the external resistor value for the LPF configuration was 300 Ω , and for the HPF configuration it was 100 Ω .

To implement the improved interface circuit, the following MOSFET transistors in SO-8 package were used: IRF7311 (dual N-MOS transistor) and IRF7307 (complementary N,P-MOS transistor). The maximal allowable continual drain current of the N-MOS transistors is 5.2 A, and -4.3 A for the P-MOS transistor. However, we assumed a maximum allowable sensor pulse current of 100 mA and therefore we choose an external resistor of 47 Ω . The experimental results are summarized in Table 1.

TABLE 1. SUMMARIZED EXPERIMENTAL RESULTS

| PARAMETER | HPF | | LPF | | HPF+MOSFET | |
|------------------|---------------------|------------------------|---------------------|------------------------|---------------------|------------------------|
| | t_x [μ s] | σ [μ s] | t_x [μ s] | σ [μ s] | t_x [μ s] | σ [μ s] |
| $L_x = 1$ mH | 8.6 | / | 3.2 | / | 18.2 | / |
| $L_x = 8.8$ mH | 77.4 | 0.06 | 27 | 0.015 | 165 | 0.19 |
| N [bits] | 8.42 | | 6.89 | | 9.52 | |
| u_q [μ s] | 0.058 | | 0.058 | | 0.058 | |
| u_n [μ s] | 0.019 | | 0.005 | | 0.06 | |
| $ENOB$ [bits] | 8.4 | | 6.8 | | 9.0 | |

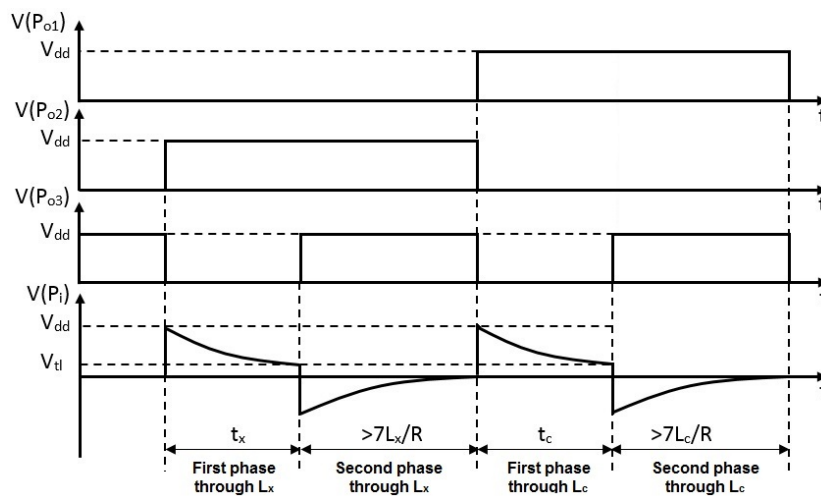


Fig. 6. Voltage waveforms at the microcontroller pins during the measurements

The measurements for each topology were performed once for the minimal sensor inductance (1 mH) and ten times for the maximal inductance (9 mH) to calculate the standard deviation (σ) and the standard deviation of the mean (u_n). Then, the resolution of the time-to-digital conversion and the ENOB were calculated according (3) and (4) respectively. In the calculations, an effective time base (for PIC16F877A) of $T_0=0.2 \mu\text{s}$ was used.



Fig. 7. Setup to test the improved direct interface circuit for inductive sensors

From the results reported in Table 1 it could be seen that the proposed interface circuit has a better measurement resolution. The ENOB increased 0.6 bits comparing to the basic HPF topology and nearly 2.2 bits comparing to the LPF topology. The resolution could be increased even more in cases where the inductive sensor allows higher maximal pulse current. Such results are even more advantageous in cases where the nominal inductance is in the order of microhenries where the basic LPF and HPF topology could be practically inapplicable due to very low resolution performance.

V. CONCLUSION

Direct inductive sensor-to-microcontroller interface is an alternative approach to interface inductive sensors without complex intermediate signal conditioning circuitry and without an analog to digital converter. To achieve this goal, a microcontroller is used to excite and measure the response of a passive RL network. One of the problems of this approach is the low-value time constant when measuring low-inductance sensors due to the limited microcontroller port sink/source current which limits the resolution of the measurements.

This paper proposes a solution to increase the discharging time constant by using external MOSFET transistors. The experimental results show that an improvement of the resolution comparing to the basic configurations can be easily achieved. Such improvement of the basic interface circuits can be very useful, especially when interfacing low-inductance sensors (say, lower than 1 mH).

REFERENCES

- [1] J. Wilson, "Capacitive and Inductive Displacement Sensors" in *Sensor Technology Handbook*, Elsevier Inc. Oxford, USA, 2005, pp. 193-222
- [2] R. P. Areny, J. Webster, "Signal Conditioning for Reactance Variation Sensors" in *Sensors and Signal Conditioning*, John Wiley & Sons Inc., Ney Work, USA, 2001, pp. 271-321
- [3] N. Philip, B. George, "Dual Slope Inductance-to-Digital Converter for Differential Reluctance Sensors", *Instrumentation and Measurement Technology Conference (I2MTC)*, Minneapolis, USA, 2013, pp. 916-919.
- [4] Y. C. Chung, N. N. Amarnath, C. M. Furse, "Capacitance and Inductance Sensor Circuits for Detecting the Lengths of Open and Short-Circuited Wires", *IEEE Trans. Instrum. Meas.*, vol. 58, pp. 2495-2502, Aug. 2009.
- [5] Texas Instruments (2013), LDC1000 Inductance to Digital Converter, Application note SNOSCX2A
- [6] Microchip Technology Inc. (2011), See What You Can Do with the CTMU, Application Note AN1372
- [7] F. Reverter, R. Pallàs-Areny, "Direct Sensor-to-Microcontroller Interface Circuits: design and characterisation," Marcombo, Barcelona, Spain, 2005
- [8] F. Reverter, O. Casas, "Interfacing Differential Capacitive Sensors to Microcontrollers: A Direct Approach", *IEEE Trans. Instrum. Meas.*, Vol. 59, pp. 2763 – 2769, Oct. 2010
- [9] F. Reverter, O. Casas, "Interfacing Differential Resistive Sensors to Microcontrollers: A Direct Approach", *IEEE Trans. Instrum. Meas.*, Vol. 58, pp. 3405 – 3410, 2009
- [10] E. Sifuentes, O. Casas, F. Reverter, and R. Pallàs-Areny, "Direct interface circuit to linearise resistive sensor bridges," *Sens. Actuators A: Phys.*, vol. 147, pp. 210-215, Sept. 2008
- [11] A. Custodio, *Contribución al diseño de interfaces de señal en sensores inteligentes* (in Spanish), PhD Thesis, Universitat Politècnica de Catalunya, Spain, 2001.
- [12] P. Yedamale, J. Bartling, See What You Can Do with the CTMU, AN1375, Microchip Technology Inc. (2011).
- [13] Z. Kokolanski, "Improving the metrological performances of digital systems based on time to digital conversion", PhD Thesis, Ss. Cyril and Methodius University in Skopje, Macedonia 2013.
- [14] Z. Kokolanski, J. Jordana, M. Gasulla, V. Dimcev, F. Reverter, "Microcontroller-based interface circuit for inductive sensors", *Procedia Engineering – Eurosensors 2014*, Vol. 87, pp. 1251-1254, 2014
- [15] Z. Kokolanski, J. Jordana, M. Gasulla, V. Dimcev, F. Reverter, "Direct inductive sensor-to-microcontroller interface circuit", *Sens. Actuators. A: Phys.*, Vol. 224, pp. 185–191, Apr. 2015
- [16] L. Zaworski, D. Chaberski, M. Kowalski, M. Zieliński, "Quantization error in time-to-digital converters", *Metrol. Meas. Syst.*, Vol. XIX, no.1, pp.115-122, 2012
- [17] E.G. Bakhoun, M.H.M. Cheng, "High-sensitivity inductive pressure sensor", *IEEE Trans. Instrum. Meas.* Vol. 60, pp. 2960-2966, 2011.